Volume 1 | Number 1 | Jan 2013 | Pages 1–100

Journal of
Materials Chemistry C

Materials for optical and electronic devices
www.rsc.org/materialsC

ROYAL SOCIETY
OF CHEMISTRY

ROYAL SOCIETY
OF CHEMISTRY

www.rsc.org/materialsC

Submitted to Journal of Materials Chemistry C

Facile fabrication of ultrathin graphene papers for effective electromagnetic shielding

Wei-Li Song,[†, §] Li-Zhen Fan,[†,*] Mao-Sheng Cao,[‡,*] Ming-Ming Lu,[‡] Chan-Yuan Wang,[‖] Jia Wang,[†] Tian-Tian Chen,[†] Yong Li,[‡] Zhi-Ling Hou,[‡,§] Jia Liu,[‡] Ya-Ping Sun[§]

[†]*Institute of Advanced Materials and Technology, University of Science and Technology Beijing, Beijing, 100083, P. R. China.*

[‡]*School of Materials Science and Engineering, Beijing Institute of Technology, Beijing, 100081, P. R. China.*

[§]*Department of Chemistry and Laboratory for Emerging Materials and Technology, Clemson University, Clemson, South Carolina 29634-0973, USA.*

[‖]*310 Department, 3rd Institution of China Aerospace Science & Industry, Beijing 100071, P. R. China.*

* Corresponding Authors: Tel/Fax: +86 10 6233-3548, +86 10 6891-4062.

Email: fanlizhen@ustb.edu.cn (Li-Zhen Fan), caomaosheng@bit.edu.cn (Mao-Sheng Cao).

Abstract: Ultrathin electromagnetic interference (EMI) shielding materials promise great application in the portable electronic devices and communication instruments. Lightweight graphene-based materials have been pursued for their exclusive microstructures and unique shielding mechanism. However, the large thickness of the current low-density graphene-based composites still limits their application potential in ultrathin devices. In this work, a novel approach has been taken to use conductive graphene paper (GP) in the fabrication of ultrathin EMI shielding materials. The as-prepared flexible GPs exhibit highly effective shielding capabilities, reaching ~19.0 dB at ~0.1 mm in thickness and ~46.3 dB at ~0.3 mm in thickness, thus the thinnest with the best shielding performance among graphene-based shielding materials. Double-layered shielding attenuators have been designed and fabricated for the high shielding performance of up to ~47.7 dB at GP thickness of ~0.1 mm. Mechanistically, the high performance should be due to Fabry-Pérot resonance, which is unusual in carbon-based shielding materials. The preparation for conductive GPs of superior shielding performance is relatively simple, amenable to large-scale production of ultrathin materials for EMI shielding and electromagnetic attenuators, with broad applications in lightweight portable electronic devices.

Keywords: graphene papers, electrically conductive, electromagnetic shielding, ultrathin

1. Introduction

The development of communication technology along with electronic devices has generated significant concerns on electromagnetic irradiations, increasing the demand for high-performance electromagnetic interference (EMI) shielding materials.[1-4] There has been much effort on the fabrication of carbon-based composites as alternative EMI shielding materials to the traditional metals, as the composites are light weight and excellent in corrosion-resistance, widely applicable in blocking and attenuating unexpected electromagnetic irradiations from electronic devices.[5,6] Apart from earlier progress with carbon nanotubes for EMI shielding,[1,2,6] graphene-based nanostructures such as graphene composite films[7] and foams[8] have attracted much recent attention for electromagnetic attenuation and reflection based on their unique two-dimensional structures and excellent electrical conductivity.

According to the fundamental mechanism of EMI shielding, enhanced shielding performance could be achieved through primarily the improvement in EMI absorption, reflection, and/or multiple reflections.[3,6,9] Exploratory studies have have demonstrated that the reflections could be improved with dispersion of graphene nanosheets into polymeric matrices.[10-15] Furthermore, porous graphene-based materials have been developed recently for the purpose of enhancing the internal random reflections.[8,10-12,16] In the graphene/polymer composite materials, the shielding performance is highly dependent on the filler loading, with a general requirement for the embedded graphene nansheets to form effective conductive interconnections.[7,8] For example, according to a recent report graphene/poly(methylmethacrylate) composite foams with a low electrical conductivity (~0.03 S cm^{-1}) were not so effective in the shielding, 13-19 dB in comparison with the commercially achievable level of >20 dB, mainly owing to the insufficient conductive network in the composite foams.[10]

There is also the relationship between the effective thickness, defined as the thickness required for the materials to achieve the shielding performance of >20 dB), and the electrical properties of the materials in EMI shielding.[3,6] For materials of relatively poor electrical properties, more materials such as in thicker sheets could be used to compensate for achieving the desired EMI shielding results.[8,10,11] Hence, the effective thicknesses of the graphene-based composite foams are mostly on the order of many millimeters or larger since the foam materials are usually low in electrical conductance.[10-12] Some researchers have attempted to compress the composite foams to decrease the shielding thickness, but the results have been a reduction in the shielding performance.[11] Although high specific shielding effectiveness (dB cm^3 g^{-1} in unit) has been pursued with these foam-like structures, the large volume and thickness of these low-density bulk materials may limit their application potential in ultrathin and flexible portable devices. In a study by Chen, *et al*., a somewhat different strategy was used to enhance the electrical conductivity in graphene/poly(dimethyl siloxane) composite foams (~2 S cm^{-1}), resulting in a smaller effective thickness (~1 mm) and a shielding effectiveness of 22-25 dB in the frequency range of 8.2-12.4 GHz.[8]

More recently, conductive composite films of graphene/poly (ethylene/vinyl acetate) were fabricated to decrease the effective thickness in EMI shielding.[7] With an electrical conductivity of ~2.5 S cm^{-1} in the composite films, similar to that in the foams discussed above, the same shielding performance (23-27 dB) could be achieved with the films of only ~0.36 mm in effective thickness.[7] Apparently, thin films/papers represent a more advantageous configuration for graphene-based composites in EMI shielding, with smaller effective thickness, good mechanic flexibility, and easy processing for broader application opportunities. Here we report a new approach to achieve superior EMI shielding results by preparing high-performance

thin graphene papers (GPs) for double-layered EMI attenuators. The preparation of the GPs was based on a conceptually different new strategy that involves no thermal reduction or thermal annealing. The GPs thus obtained were highly conductive, up to 220 S cm^{-1}, higher than those found in most of the chemically converted graphene oxide (GO) papers. At ~0.3 mm in thickness, the GPs exhibited EMI shielding performance of ~46.3 dB, probably representing the thinnest graphene material for the same shielding effectiveness. Further performance enhancement was achieved with the double-layered EMI attenuators fabricated from thinner GPs (~0.1 mm in thickness). The mechanistically distinctive enhancement due to the formation of Fabry-Pérot capacity has been rather rarely in carbon-based shielding materials. The results demonstrate new opportunities in the use of graphene for rationally designing and fabricating high-performance EMI shielding materials and electromagnetic attenuators.

2. Results and discussion

In the literature electrically conductive graphene papers were mostly prepared as reduced GO (rGO) papers, namely through the conversion of the initial insulating GO papers to recover substantial electrical conductivity (Figure S1a).[17-24] Since the preparation of GOs involves exhaustive oxidation processes, severely damaging the electrical properties, their subsequent recovery requires elaborate processing steps including chemical reduction and high-temperature thermal annealing in hydrogen-rich or inert atmosphere.[17-24] In this study the electrically conductive graphene papers (GP) were fabricated directly from the multilayered graphene (MLG) sheets, for which the preparation method was reported previously.[26,27] The direct approach is more suitable for eventual large-scale production, eliminating the recovery processes in the

conversion of GO papers and their associated uses of toxic reagents and the significant loss of the paper materials. [17,19,23,24]

Aqueous suspension of MLG (Figure 1a) was prepared as reported previously.[26,27] In brief (Figure S1b), the as-received graphite sample was pre-treated in an aqueous alcohol solution and subsequently exfoliated in mixed acids. The as-treated samples were dispersed into water for repeated washing until the pH of the aqueous suspension reached neutral. A portion of the final aqueous suspension of the MLG was diluted for direct filtration to result in a GP on the filter. The originally formed GPs could be re-processed. In the process, the as-prepared original GPs were re-dispersed into aqueous solution with the needle-sonication. The well-dispersed aqueous suspension (Figure S2a) was used for the flow-filtration to yield a re-processed GP. Both the originally formed GP (Figure 1b) and re-processed GP (Figure S2a) were free-standing and mechanically flexible.

According to SEM imaging results, the GPs were stacked with highly aligned MLG nanosheets (Figure 1c). The TEM image for a typical MLG piece (Figure 1d) suggested that its planar size was in several microns. Results from the TEM imaging of the microtomed specimen for a cross-sectional view suggested that the MLG sheets of mostly 3-5 nm in thickness were stacked into a highly aligned layered configuration (Figure 1e and 1f), representing the primary structure in the flexible GPs. The aspect ratio for the MLG sheets was estimated at 1000 or higher. The high aspect ratio along with aligned layered structure in the conductive GPs should be ideal to the directed electromagnetic reflections. Additionally, the re-processed GPs were structurally similar to the original GPs (Figure S2b). According to the XRD patterns and the peak broadening (Figure 2a), the reprocessing had no significant impact on the morphology and structure of the exfoliated MLG sheets, with the estimated average MLG thickness (according to

Scherrer Equation) in re-processed GPs (~8.4 nm) close to that (~7.8 nm) in the original GPs. Furthermore, the result of mechanical properties shows the greatest mean tensile strength up to ~246 MPa in the original GPs, indicating that mechanically robust GPs could be achieved (Figure 2b).

The electrical conductivity/surface resistance of the GPs was measured by using the four-probe method. The surface resistance for both the original and reprocessed GPs was between 0.85-0.95 Ohm sq^{-1} (Figure 2c), corresponding to electrical conductivity of 180-220 S cm^{-1} (Figure 2c). The conductivity values are much higher than those found in most of the chemically converted GO papers[17,19,20,22,23] and close to the best level achieved in the thermally annealed GO papers (Figure S3).[17-20,22,23,25]

Fourier transform infrared spectroscopy (FTIR) was applied to both GPs and graphite samples (Figure 3a), suggesting that the GPs present very similar spectra to graphite. In the GP spectra, the peaks at 1610 cm^{-1} and 1700 cm^{-1} are assigned to the stretch of C=C and C=O, respectively.[28] The peak observed around 3230 cm^{-1} and broad peaks around 3400~3560 cm^{-1} could be associated with the stretching vibration of N-H and O-H, respectively.[28] The broad peaks 1000~1300 cm^{-1} in the fingerprint region should refer to the overlap of stretching vibrations from C-C, C-O and C-N.[28] For further characterization, X-ray photoelectron spectroscopy (XPS) was used to determine the components of the GPs (Figure 3b). The elemental concentrations of C, N and O in the GP were 90.36%, 0.93% and 8.71%, respectively (Table S1), and the C:O ratio of 10.37 (Table S1) was higher than those found in the conventional hydrazine-reduced[25,29] and thermally reduced[25] GO papers, as well as those from other chemical conversions.[29] In the C1s spectrum of the GP (Figure 3c), pronounced peaks were observed at 284.8 eV, 286.1 eV and 287.8 eV, corresponding to carbon-carbon, C–O, and C=O

species, respectively.[30] Compared to the as-received graphite sample, the slight shift in the carbon-carbon peak indicates partial conversion of sp^2 hybridization into sp^3 hybridization in the exfoliation process (Figure 3d).[29,31] According to Raman spectrum (Figure 2d), the peak located at ~1585 cm^{-1} was assigned as the G-band, representing the characteristic of the sp^2-hybridized carbon-carbon bonds in graphene sheets.[32,33] The peak observed at ~1350 cm^{-1} (D-band) refers to the structural imperfections caused by the presence of functional groups on the carbon plane.[32,33] The 2D-band peak centered at ~2700 cm^{-1} is known as the second-order Raman feature of the D-band and is associated with a double resonance process.[33] Additionally, the intensity ratio between the D-band and G-band was around 0.36, much smaller than those found in the conventional chemically converted and thermally annealed GO papers.[23,34] The FTIR, XPS and Raman results collectively suggested that the graphitic structure responsible for the electrical conductivity was largely preserved in the processing for MLG and the fabrication for GPs.

The fabrication of the electrically conductive GPs in this study was obviously different from those procedures based on reduced GO papers (Figure S1), where the harsh oxidation conditions for GOs destroy the electrical conductivity completely, whose recovery is complicated and generally inefficient. Therefore, the direct approach is more advantageous.

As suggested recently, the hydrogen bonding network between hydrophilic groups and water and the compression from the air-water interface are considered as two major factors in the formation of highly aligned GO papers.[35] Similarly, the presence of water increases the degrees of freedom for the MLG sheets due to the creation of hydrogen bond network via water and hydrophilic groups (-OH and -COOH) on the MLG surface, which in turn improves the ability for the MLG sheets to disperse. In the filtration processing, the compressive force due to the decrease of air-water interface serves to reduce the MLG spacing and simultaneously aligns the

MLG sheets to the air-water interface. With the vigorous mechanical forces to break the molecular interactions between stacked MLG sheets, the insertion of water into the MLG spacing facilitates the re-dispersion of the MLG sheets via the reconstruction of hydrogen bonding network, allowing further filtration for re-processed GPs.

A layered structure of the GP sandwiched in wax substrates (wax|GP|wax, Figure 4a) was fabricated. The S parameters (S_{11} and S_{21}) for the GP were measured to evaluate the EMI shielding effectiveness (SE) in 8.2-12.4 GHz (X-band). As shown in Figure 5, insufficient SE performance (<20 dB) in the sample with GP thickness ~0.05 mm (wax|GP×1|wax, Figure 4b) could be due to the fact that the GP thickness is close to the calculated skin depth (0.03~0.04 mm, Figure S4). Thus, the electromagnetic waves may not be completed blocked or reflected by the GP of thickness ~0.05 mm since they may still penetrate through such GP. Moreover, there is a pronounced peak in the EMI shielding effectiveness of wax|GP×1|wax. Such unique peak has not been observed in the polymeric samples of insufficient SE, where MLG has been homogeneously dispersed.[7] This should refer to the enhanced anisotropic GPs formed by the highly aligned MLG stacking, which may impact the multiple reflections (if occurs in such GPs). When the thickness of the GP layer increased to ~0.1 mm (wax|GP×2|wax, Figure 4c), which is much larger than the calculated skin depth (0.03~0.04 mm), unexpected multiple reflections (if occurs in such GPs) could be also greatly diminished since the shielding effectiveness absorption was mostly greater than 10 dB (Figure 5b).[6,7] As expected, the wax|GP×2|wax sample was found to have overall EMI shielding values of 19 - 20 dB (Figure 5a), thus among the thinnest graphene-based materials (GP thickness ~0.1 mm) for the effective shielding of ~20 dB (Figure 6).[7,8,10-13] In the sample with GP thickness ~0.3 mm (wax|GP×6|wax, Figure 4d), the optimal EMI shielding was up to 46.3 dB (>99.99% shielding efficiency). This must be the thinnest

among previously reported graphene-based shielding materials for the highest shielding performance (>46 dB, Figure 6).[7,8,10-14]

In further development, a symmetric double layered structure of two GP pieces sandwiching wax (GP|wax|GP) was fabricated to serve as an electromagnetic attenuator (Figure 4e). In comparison with wax|GP×2|wax (Figure 7a) of the same components but different arrangement in the layered structures, the GP|wax(2 mm)|GP attenuator with overall thickness of the GPs ~0.1 mm (Figure 4f) exhibited a strong resonance peak, corresponding to a dramatic enhancement in shielding effectiveness to 47.7 dB (Figure 7a). This EMI absorption value is almost 3-fold higher than that in wax|GP×2|wax sample (Figure 7b). Such unusual absorption peak is attributed mainly to the formation of Fabry-Pérot cavity resonance.[36,37] In a typical Fabry-Pérot cavity, multiple reflections could be aligned between parallel reflecting GP planes, producing constructive interference when the reflected waves are in phase. Therefore, the corresponding shielding effectiveness reflection in GP|wax|GP attenuator was largely suppressed (Figure 7c), leading to a much higher absorption efficiency in comparison with that in the wax|GP×2|wax configuration (Figure 7d).

The thickness of the wax spacing between two reflecting GPs in the attenuators was varied, and its effect on the attenuator performance was evaluated. As expected, the observed resonance peak was shifted toward lower frequency with increasing wax spacing (Figure 8a and 8b), which might be rationalized in term of the resonance at a longer wavelength requiring a larger distance for the occurrence of constructive interference. This actually enables a promising strategy in the design of electromagnetic attenuating devices to tune the resonance peak via altering the spacing thickness.

The enhanced attenuating mechanism based on Fabry-Pérot resonance is completely different from the mostly random internal reflections observed in other graphene-based shielding materials.[7,8,10-14] In fact, the Fabry-Pérot resonance is rarely observed in carbon-based EMI shielding materials,[1,2,6-8,10-16] including in similar layered structures formed by CNT papers.[38] The optimal performance (~47.7 dB) of the GP|wax(2 mm)|GP attenuator with ~0.1 mm in the total GP thickness is significantly higher than that achieved with other graphene-based shielding materials over the same frequency range (Figure 6),[7,8,10-14] and competes well with those of many-times thicker CNT-based (Figure S5a) and metal-based bulk materials (Figure S5b). These ultrathin EMI materials in the attenuator configuration of record-setting shielding effectiveness may find a variety of uses, such as in thin shielding coatings or smart electromagnetic attenuating devices. The concept based on the highly efficient absorption generated by the graphene-based Fabry-Pérot cavity could be further developed in the design and fabrication of novel graphene-based metamaterials and devices for even broader applications. [36,37]

3. Conclusion

In summary, a novel direct fabrication approach was used for the GPs of high electrical conductivity. The as-prepared GPs were found to be highly effective electromagnetic shielding, reaching ~46.3 dB at a thickness of ~0.3 mm, thus among the thinnest graphene-based materials for the performance. In the double-layered attenuator configuration with the GPs, much enhanced absorption due to the Fabry-Pérot resonance was observed, achieving the record-setting shielding effectiveness of ~47.7 dB with only ~0.1 mm in the total GP thickness. The ultrathin GP-based materials and devices of superior EMI shielding performance, with

advantages also including light weight and mechanical flexibility, will prove valuable in a variety of applications.

4. Experimental Section

GPs: The strategy for graphene papers (GP) was developed based on our previous methods for preparing MLG.[26,27] The aqueous MLG suspension was firstly obtained. In a typical experiment, the commercial graphite sample (0.5 g) (surface enhanced flake graphite, grade 3805 from Asbury Carbons) was pre-treated in alcohol aqueous. The pre-treated samples were dried in vacuum oven, followed by oxidative acid treatment in a mixed acid solution (20 ml nitric acid and 60 ml sulfuric acid) under sonication for 48-72 h. The resulting samples were transferred to 2L water and diluted with abundant water. Subsequently, a portion of the diluted aqueous suspension was treated in sonication for 1h and then transferred into the filtration to achieve GP. The as-fabricated GP was dried in a vacuum oven and then peeled off for further characterization and measurements.

Re-processed GPs: A portion of the as-prepared original GP was positioned in 40 ml water. A vigorous needle-sonication was utilized to re-disperse the GP paper in the water until no precipitation was observed. Subsequently, the as-treated suspension was treated in sonication for another 2h. The resulting well-dispersed suspension was re-filtered to achieve re-processed GPs.

Layered structures (wax/GP/wax): In the fabrication of the wax substrates (Figure 4a), paraffin wax (~200 mg) was compressed into a cubic sheet with dimensions of $22.86 \times 10.16 \times 1 \ mm^3$ (size of testing chamber). On the other hand, ethylene-vinyl acetate copolymers (EVA) was dissolved toluene, followed by evaporating most of solvent to obtain viscous EVA/toluene glue. To ensure the consistency, all the measured GPs were re-processed from ~50 mg original GPs,

followed by cutting into rectangular shape of 22.86×10.16 mm^2. All the rectangular GP thin papers were about 40-50 microns in thickness with ~8 mg in weight.

In the fabrication of wax|GP|wax structures, the resulting EVA/toluene glue was cast onto one piece of the as-prepared wax substrate and then was pasted with the GP to form GP|wax structure (Figure 4a). The EVA/toluene glue was subsequently cast on the GP|wax structure, followed by pasting the other piece of wax substrate to achieve a wax|GP|wax layered structure. Similarly, the other wax|GP|wax structures with different GP pieces (2 and 6 pieces) were also fabricated (Figure 4c and 4d). All the wax|GP|wax structures were dried in an ambient condition to achieve testing samples.

GP Attenuators *(GP|wax|GP):* As shown in Figure 4e, symmetric double layered attenuators (GP|wax|GP) were fabricated via the similar procedure described above. The thicknesses of the wax spacing in GP|wax|GP attenuators are 2, 3, 4, 5 mm (Figure 4f-4i).

EMI shielding*:* The *S* parameters (S_{11} and S_{21}) of the as-fabricated wax|GP|wax structures and GP|wax|GP attenuators were measured on an Anritsu 37269D vector network analyzer (VNA) using the wave guide method in X-band.[7] The power coefficients, reflection coefficient (*R*) and transmission coefficient (*T*), were calculated by the equations of $R=|S_{11}|^2$ and $T=|S_{21}|^2$, respectively. Absorption coefficient (*A*) was obtained from the relation of *A=1-R-T*.[7,9] Absorption efficiency (AE) was calculated by the relation of AE=$A/(1-R)\times100\%$. EMI shielding effectiveness (SE_{tot}) refers to the logarithm of the ratio of the incident wave P_I to the transmitted wave P_T, which is determined by the equation of $SE_{tot}=10\log(P_I/P_T)$dB. The total experimental SE is the sum of the net shielding by reflection (SE_{ref}) and absorption (SE_{abs}), which can be given as $SE_{ref}=-10\log(1-R)$dB and $SE_{abs}=-10\log(T/(1-R))$dB, respectively.[7] For roughly estimating

skin depth of GPs, skin depth (δ) was calculated according to the relation of $\delta=(\pi\sigma f\mu)^{-1/2}$, where σ is the electrical conductivity, f the frequency and μ the magnetic permeability.[6,7]

Characterizations: The as-achieved GPs were applied to X-ray diffraction (XRD) characterization on a PANalytical X' Pert PRO MPD diffraction system. X-ray photoelectron spectra (XPS) of the GPs were recorded using a K-alpha on Thermo Fisher Scientific ESCALAB 250xi system. Fourier transform infrared spectroscopy (FTIR) was performed on a Nicolet 8700 FTIR system. Raman spectra were performed on a Jobin Yvon T64000 Raman spectrometer equipped with a Melles-Griot 35 mW He-Ne laser source for 633 nm excitation. Field emission scanning electron microscopy (SEM) was carried out on a ZEISS supra 55 system. Transmission electron microscopy (TEM) images were obtained on a Hitachi HD-2000 Scanning-TEM system and a Hitachi H-9500 TEM system. In the preparation of TEM specimens by microtoming, powder samples were embedded in epoxy resin, followed by the use of a Reichert-Jung Ultracut E Microtome with a 30 °angle diamond knife at room temperature for slices (cross-sectional with respect to the original film) of less than 100 nm in thickness. Static in-plane tensile tests were carried out with a mechanical analyzer (TA-XT Plus system, SMS) and the GP was cut into rectangular strips of approximately 1×20 mm^2 for mechanical testing. The surface resistance (R_s) and electrical conductivity (σ) was determined using the classical four-probe method, with the electrical current (I) and voltage (V) relationship for the GPs obtained by a multimeter (Keithley 2400, controlled by Lab Tracer 2.0 software, both from Keithley Instruments) and a multiheight probe (Jandel). The surface resistance could be calculated based on the relation of $R_s = (\pi/\ln 2)(V/I)$. With the relation of GP thickness (d), the electrical conductivity for the GPs was determined by the equation $\sigma = (\ln 2/\pi)(I/V)/d$.

-15-

Acknowledgements

References

[1] N. Li, Y. Huang, F. Du, X. B. He, X. Lin, H. J. Gao, Y. F. Ma, F. F. Li, Y. S. Chen, P. C. Eklund, *Nano Lett.* 2006, **6,** 1141.

[2] Y. L. Yang, M. C. Gupta, K. L. Dudley, R. W. Lawrence, *Nano Lett*. 2005, **5**, 2131.

[3] D. D. L. Chung, *Carbon* 2001, **39**, 279.

[4] H. J. Yang, M. S. Cao, Y. Li, H. L. Shi, Z. L. Hou, X. Y. Fang, H. B. Jin, W. Z. Wang, J. Yuan, *Adv. Optical Mater.* 2013, DOI: 10.1002/adom.201300439.

[5] D. D. L. Chung, *Carbon* 2012, **50**, 3342.

[6] M. H. Al-Saleh, U. Sundararaj, *Carbon* 2009, **47**, 1738.

[7] W. L. Song, M. S. Cao, M. M. Lu, S. Bi, C. Y. Wang, J. Liu, J. Yuan, L. Z. Fan, *Carbon* 2014, **66**, 67.

[8] Z. P. Chen, C. Xu, C. Q. Ma, W. C. Ren, H. M. Cheng, *Adv. Mater.* 2013, **25**, 1296.

[9] M. S. Cao, W. L. Song, Z. L. Hou, B. Wen, J. Yuan, *Carbon* 2010, **48**, 788.

[10] H. B. Zhang, Q. Yan, W. G. Zheng, Z. X. He, Z. Z. Yu, *ACS Appl. Mater. Interfaces* 2011, **3**, 918.

[11] J. Q. Ling, W. T. Zhai, W. W. Feng, B. Shen, J. F. Zhang, W. G. Zheng, *ACS Appl. Mater. Interfaces* 2013, **5**, 2677.

[12] D. X. Yan, P. G. Ren, H. Pang, Q. Fu, M. B. Yang, Z. M. Li, *J. Mater. Chem.* 2012, **22**, 18772.

[13] S. Maiti, N. K. Shrivastava, S. Suin, B. B. Khatua, *ACS Appl. Mater. Interfaces* 2013, **5**, 4712.

[14] J. J. Liang, Y. Wang, Y. Huang, Y. F. Ma, Z. F. Liu, J. M. Cai, C. D. Zhang, H. J. Gao, Y. S. Chen, *Carbon* 2009, **47**, 922.

[15] A. P. Singh, P. Garg, F. Alam, K. Singh, R. B. Mathur, R. P. Tandon, A. Chandra, S. K. Dhawan, *Carbon* 2012, **50**, 3868.

[16] Q. L. Liu, J. J. Gu, W. Zhang, Y. Miyamoto, Z. X. Chen, D. Zhang, *J. Mater. Chem.* 2012, **22**, 21183.

[17] S. Park, R. S. Ruoff, *Nat. Nanotechnol.* 2009, **4**, 217.

[18] H. Chen, M. B. Muller, K. J. Gilmore, G. G. Wallace, D. Li, *Adv. Mater.* 2008, **20**, 3557.

[19] D. Li, M. B. Muller, S. Gilje, R. B. Kaner, G. G. Wallace, *Nat. Nanotechnol.* 2008, **3**, 101.

[20] W. Gao, L. B. Alemany, L. J. Ci, P. M. Ajayan, *Nat. Chem.* 2009, **1**, 403.

[21] S. Dubin, S. Gilje, K. Wang, V. C. Tung, K. Cha, A. S. Hall, J. Farrar, R. Varshneya, Y. Yang, R. B. Kaner, *ACS Nano* 2010, **4**, 3845.

[22] X. Zhao, C. M. Hayner, M. C. Kung, H. H. Kung, *ACS Nano* 2011, **5**, 8739.

[23] X. Y. Lin, X. Shen, Q. B. Zheng, N. Yousefi, L. Ye, Y. W. Mai, J. K. Kim, *ACS Nano* 2012, **6**, 10708.

[24] S. F. Pei, J. P. Zhao, J. H. Du, W. C. Ren, H. M. Cheng, *Carbon* 2010, **48**, 4466.

[25] C. Vallés, J. D. Núñez, A. M. Benito, W. K. Maser, *Carbon* 2012, **50**, 835.

[26] L. M. Veca, M. J. Meziani, W. Wang, X. Wang, F. Lu, P. Zhang, Y. Lin, R. Fee, J. W. Connell, Y. P. Sun, *Adv. Mater.* 2009, **21**, 2088.

[27] W. L. Song, W. Wang, L. M. Veca, C. Y. Kong, M. S. Cao, P. Wang, M. J. Meziani, H. J. Qian, G. E. LeCroy, L. Cao, Y. P. Sun, *J. Mater. Chem.* 2012, **22**, 17133.

[28] R. M. Silverstein, G. C. Bassler, T. C. Morrill, *Spectrometric Identification of Organic Compounds*, John Wiley and Sons, New York, 4th edn., 1981.

[29] A. Hunt, D. A. Dikin, E. Z. Kurmaev, T. D. Boyko, P. Bazylewski, G. S. Chang, A. Moewes, *Adv. Funct. Mater.* 2012, **22**, 3950.

[30] S. Stankovich, D. A. Dikin, R. D. Piner, K. A. Kohlhaas, A. Kleinhammes, Y. Jia, Y. Wu, S. T. Nguyen, R. S. Ruoff, *Carbon* 2007, **45**, 1558.

[31] R. Haerle, E. Riedo, A. Pasquarello, A. Baldereschi, *Phys. Rev. B* 2001, **65**, 045101.

[32] A. C. Ferrari, J. C. Meyer, V. Scardaci, C. Casiraghi, M. Lazzeri, F. Mauri, S. Piscanec, D. Jiang, K. S. Novoselov, S. Roth, A. K. Geim, *Phys. Rev. Lett.* 2006, **97**, 187401.

[33] A. Gupta, G. Chen, P. Joshi, S. Tadigadapa, P.C. Eklund, *Nano Lett.* 2006, **6**, 2667.

[34] Y. X. Xu, H. Bai, G. Lu, C. Li, G. Q. Shi, *J. Am. Chem. Soc.* 2008, **130**, 5856.

[35] K. W. Putz, O. C. Compton, C. Segar, Z. An, S. B. T. Nguyen, L. C. Brinson, *ACS Nano* 2011, **5**, 6601.

[36] X. L. Liu, T. Tyler, T. Starr, A. F. Starr, N. M. Jokerst, W. J. Padilla, *Phys. Rev. Lett.* 2011, **107**, 045901.

[37] X. L. Liu, T. Starr, A. F. Starr, W. J. Padilla, *Phys. Rev. Lett.* 2010, **104**, 207403.

[38] J. G. Park, J. Louis, Q. Cheng, J. W. Bao, J. Smithyman, R. Liang, B. Wang, C. Zhang, J. S. Brooks, L. Kramer, P. Fanchasis, D. Dorough, *Nanotechnol*. 2009, **20**, 415702.

Figure captions

Figure 1. Aqueous suspension of MLG sheets (a) and resulting flexible GP (b); Typical SEM images of GP (c); TEM image of the MLG sheet (d) and microtomed images for cross-section view of the GP (e) and (f).

Figure 2. XRD spectra of the original GP and re-processed GP (a); Typical stress–strain curve of the original GP (b); Surface resistivity and corresponding electrical conductivity of the GPs (c); Raman spectrum of GPs (d).

Figure 3. FTIR transmittance spectra of GP and graphite samples (a); XPS spectra of GP and as-received graphite sample (b); C1s spectrum of the GP (c); Comparison in C1s spectra of GP and graphite samples (d).

Figure 4. Scheme of preparing GP layered structures (a); Structures of wax|GP×1|wax (b), wax|GP×2|wax (c) and wax|GP×6|wax (d); Scheme of preparing symmetric double layered attenuator (e); Structures of GP|2 mm wax|GP (f), GP|3 mm wax|GP (g), GP|4 mm wax|GP (h) and GP|5 mm wax|GP (i).

Figure 5. Total EMI SE (b), SE absorption (c) and SE reflection (d) of the layered structures with different stacked GPs.

Figure 6. Optimal EMI SE performance with shielding thickness in recent graphene-based shielding materials.

Figure 7. Total EMI SE (a), SE absorption (b), SE reflection (c) and absorption efficiency (d) of wax|GP×2|wax sample and GP|2 mm wax|GP attenuator.

Figure 8. Total EMI SE (a) and SE absorption (b) of GP attenuators: GP|2 mm wax|GP (-□-), GP|3 mm wax|GP (-○-), GP|4 mm wax|GP (-Δ-) and GP|5 mm wax|GP (-◊-).

Figure 1.
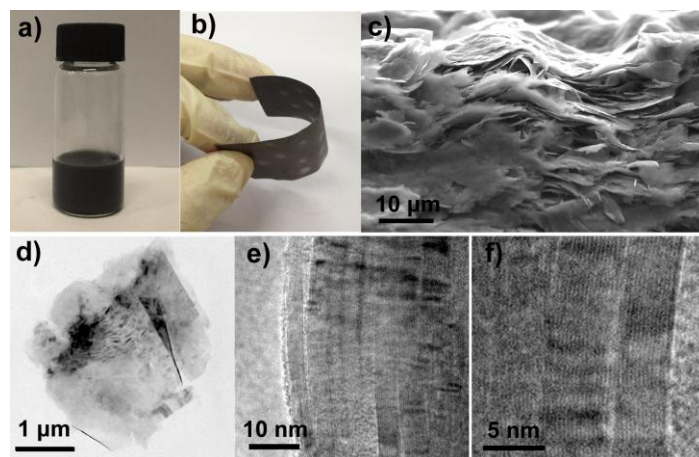
Figure 2.

Figure 3.

Figure 4.

a) Wax Substrate / EVA Glue layer / GP / GP Layered Structure (wax|GP|wax)

b) Wax / GP / Wax / 40~50 µm / (wax|GPx1|wax)

c) Wax / GP x2 / Wax / (wax|GPx2|wax)

d) Wax / GP x6 / Wax / (wax|GPx6|wax)

e) GP / EVA Glue layer / Wax Substrate / Symmetric Double Layered Attenuator (GP|wax|GP)

f) GP 40~50 µm / Wax 2 mm / GP / (GP|2 mm wax|GP)

g) GP / Wax 3 mm / GP / (GP|3 mm wax|GP)

h) GP / Wax 4 mm / GP / (GP|4 mm wax|GP)

i) GP / Wax 5 mm / GP / (GP|5 mm wax|GP)
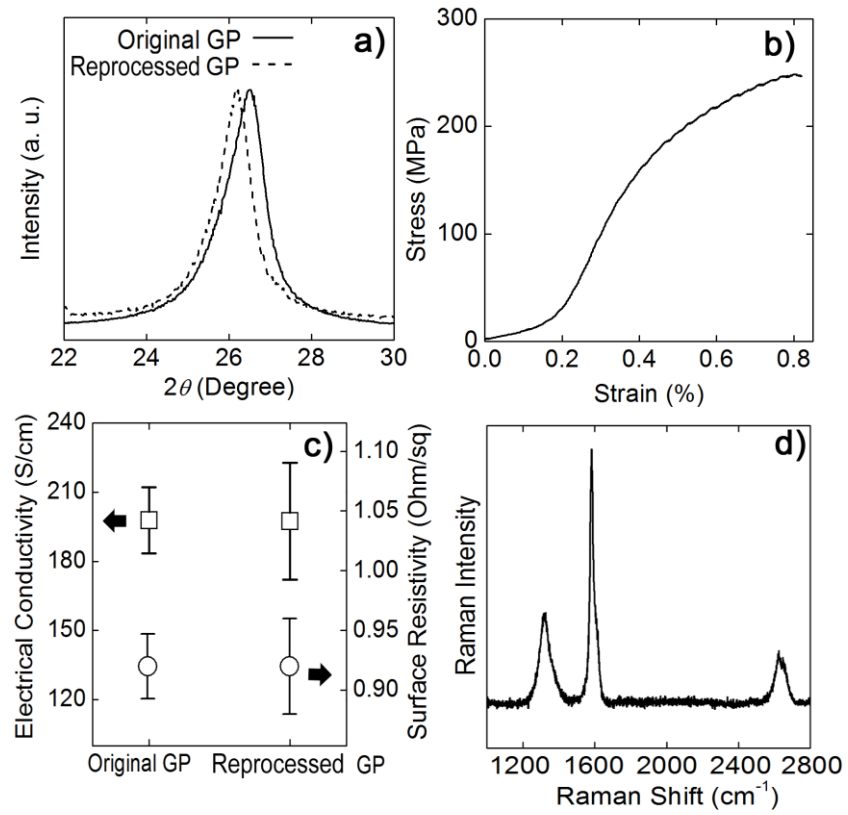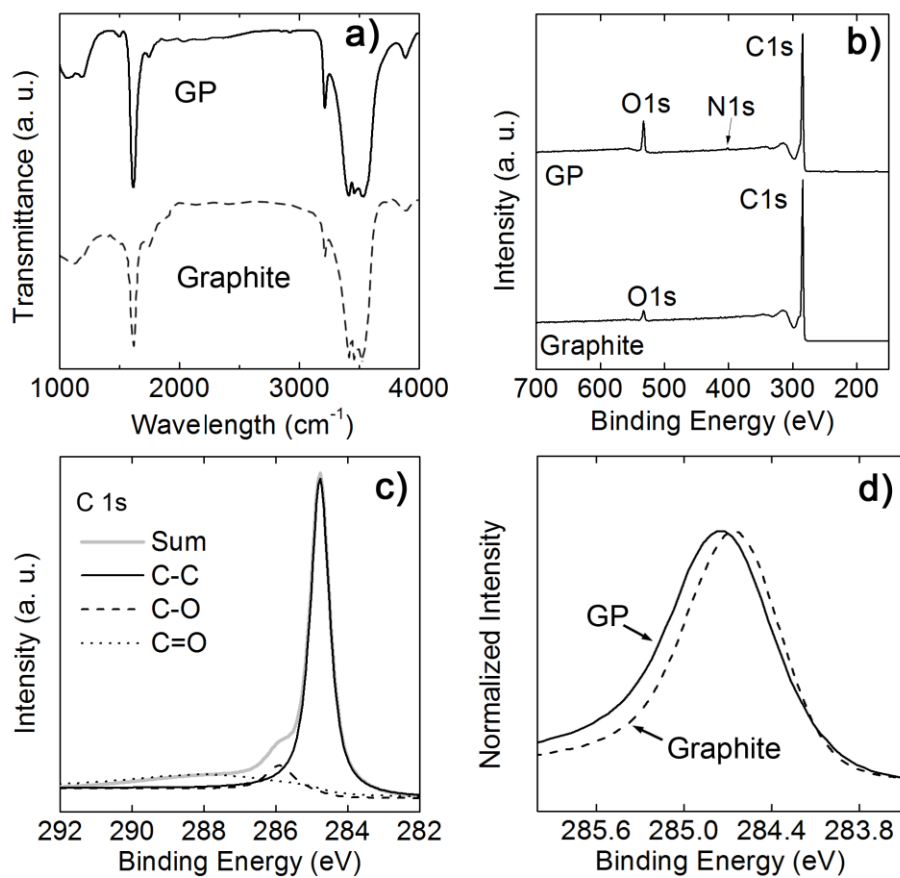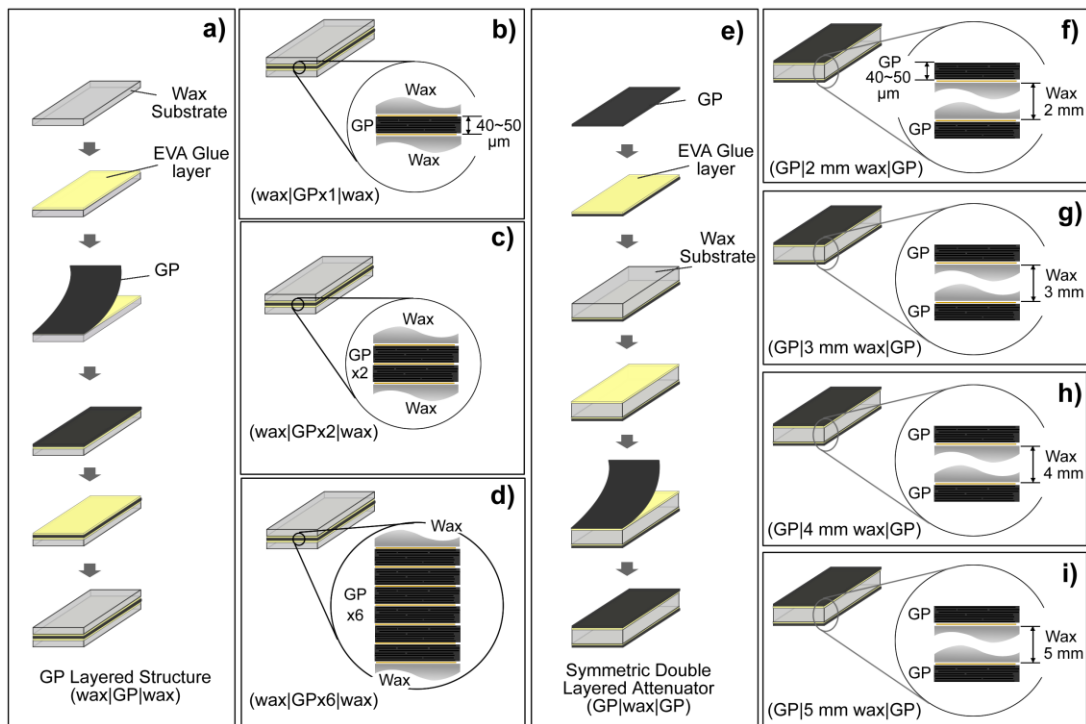
Figure 5.

-25-
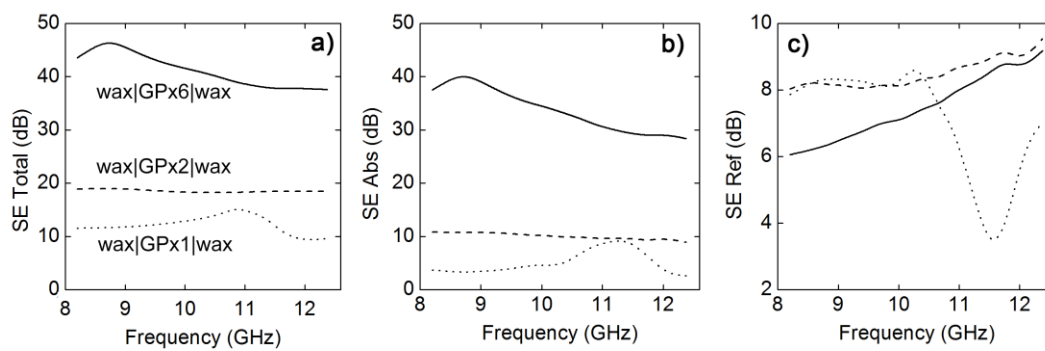
Figure 6.

Figure 7.

Figure 8.

ToC
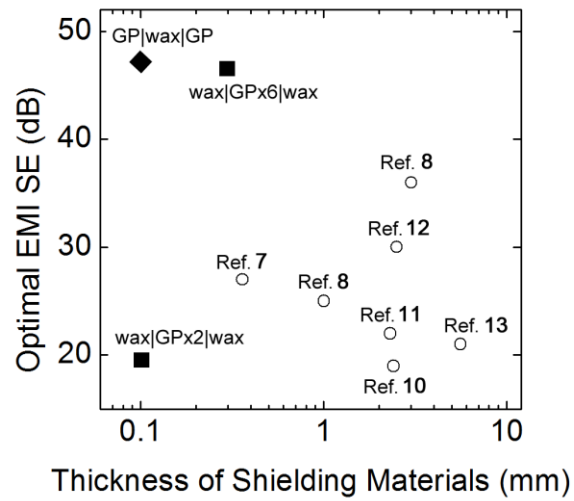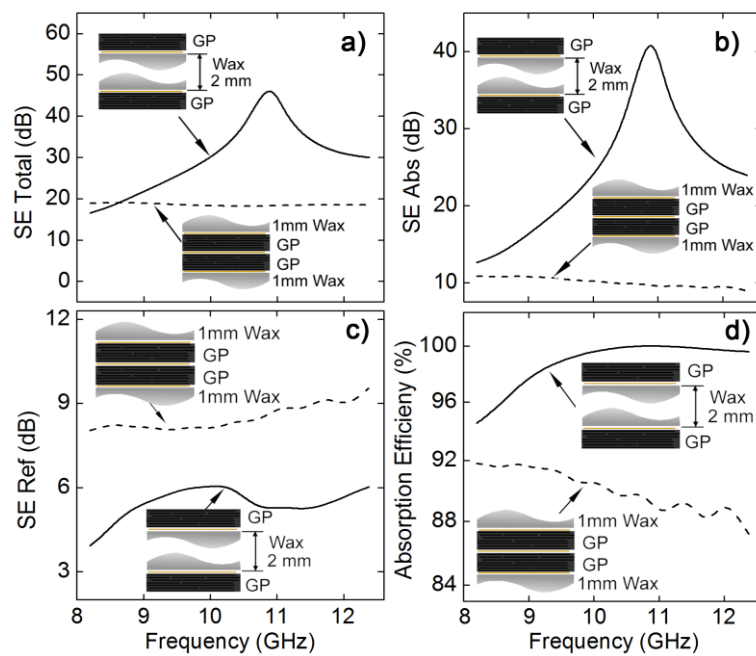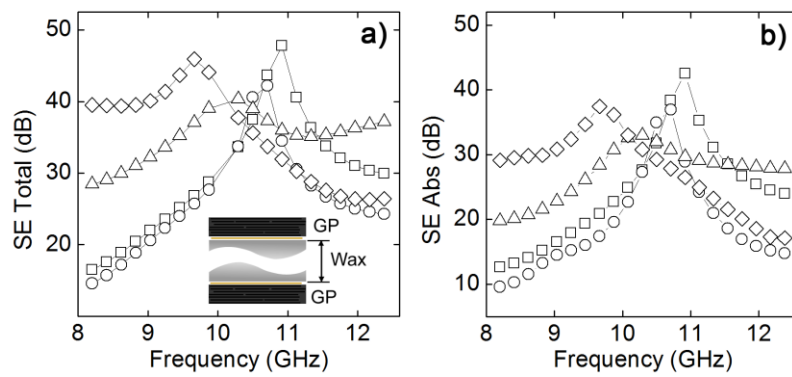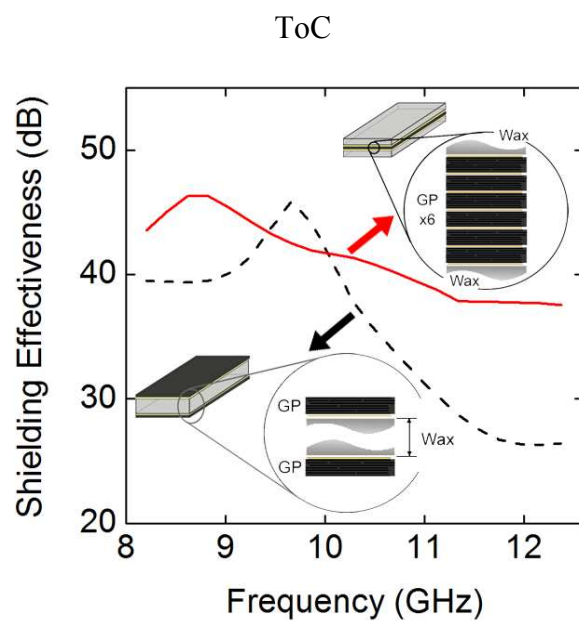
Novel conductive ultrathin graphene papers demonstrate effective EMI shielding ~46.3 dB (~0.3 mm) and ~47.7 dB ~0.1 mm in attenuators.